Terpenoids from Leaves of *Guarea macrophylla* Display *In Vitro* Cytotoxic Activity and Induce Apoptosis In Melanoma Cells

DOI 10.1055/s-0043-107241
Planta Med

Publishing House and Copyright:
© 2017 by
Georg Thieme Verlag KG
Rüdigerstraße 14
70469 Stuttgart
ISSN 0032-0943

Thieme

Terpenoids from Leaves of *Guarea macrophylla* Display *In Vitro* Cytotoxic Activity and Induce Apoptosis In Melanoma Cells

Authors

Geanne Alexandra A. Conserva[1,2], Natalia Girola[3], Carlos R. Figueiredo[3,4], Ricardo A. Azevedo[5], Sasha Mousdell[4], Patricia Sartorelli[1], Marisi G. Soares[6], Guilherme M. Antar[7], João Henrique G. Lago[2]

Affiliations

1 Instituto de Ciências Ambientais, Químicas e Farmacêuticas, Universidade Federal de São Paulo, Brazil
2 Centro de Ciências Naturais e Humanas, Universidade Federal do ABC, Santo Andre, Brazil
3 Departamento de Microbiologia, Imunologia e Parasitologia,Universidade Federal de São Paulo, Brazil
4 Department of Molecular and Clinical Cancer Medicine, University of Liverpool, United Kingdom
5 Laboratório de Imunologia de Tumores, Instituto de Ciências Biomédicas, Universidade de São Paulo, Brazil
6 Instituto de Química, Universidade Federal de Alfenas, Brazil
7 Departamento de Botânica, Instituto de Biociências, Universidade de São Paulo, Brazil

Key words

Guarea macrophylla, Meliaceae, cycloartane triterpene, isopimarane diterpene, cytotoxicity, cancer cells, apoptosis

received November 12, 2016
revised February 7, 2017
accepted March 20, 2017

Bibliography

DOI http://dx.doi.org/10.1055/s-0043-107241
Published online | Planta Med © Georg Thieme Verlag KG Stuttgart · New York | ISSN 0032-0943

Correspondence

Prof. Dr. João Henrique G. Lago
Centro de Ciências Naturais e Humanas, Universidade Federal do ABC
Av dos Estados, 5001, 09210-580, Santo André, São Paulo, Brazil
Phone: + 55 11 49 96 79 14, Fax: + 55 11 49 96 79 14
joao.lago@ufabc.edu.br

Supporting information available online at http://www.thieme-connect.de/products

ABSTRACT

Guarea macrophylla is a Brazilian plant species that has been used in folk medicine to treat a range of diseases. Our ongoing work focuses on the discovery of new bioactive natural products derived from Brazilian flora. The current study describes the identification of cytotoxic compounds from the EtOH extract of leaves from *G. macrophylla* using bioactivity-guided fractionation. This approach resulted in the isolation and characterization of four compounds: cycloart-23*E*-ene-3*β*,25-diol (**1**), (23*S**,24*S**)-dihydroxycicloart-25-en-3-one (**2**), isopimara-7,15-diene-2*α*,3*β*-diol (**3**), and isopimara-7,15-dien-3*β*-ol (**4**), in which **2** and **3** are identified as new derivatives. *In vitro* assays were conducted to evaluate the cytotoxic activity of compounds **1**–**4** against a panel of cancer cell lines and to determine the possible mechanism(s) related to the activity of the compounds on B16F10Nex2 cells. The most active compound **1** induced cytotoxic effects on tumor cells, with IC_{50} values of 18.3, 52.1, and 58.9 µM against HL-60, HeLa, and B16F10-Nex2 tumor cells, respectively. Furthermore, it was observed in melanoma cells that compound **1** induced several specific apoptotic hallmarks, such as morphological changes in the cell shape structure, nuclear DNA condensation, specific chromatin fragmentation, and disruption in the mitochondrial membrane potential, which are related to the intrinsic apoptotic pathway.

Introduction

Guarea macrophylla Vahl. ssp. Tuberculata (Meliaceae) is a tree grown in Brazil from Rio Grande do Sul to Minas Gerais States and in the Amazon region. It has been used in folk medicine to treat different maladies such as inflammations and diarrhea as well as acting as a depurative agent [1]. Despite several chemical studies on *G. macrophylla* in which different terpenoids have been characterized [2, 3], there are no reports in the literature describing the bioactivity associated to this plant. As part of our studies on the discovery of antitumor metabolites from Brazilian plant species [4], the EtOH extract from leaves of *G. macrophylla* were examined to identify compounds that display cytotoxic activity against a panel of cancer cell lineages (B16F2Nex2, A2058, MCF7, HL-60, and HeLa). In this paper, we report the isolation of

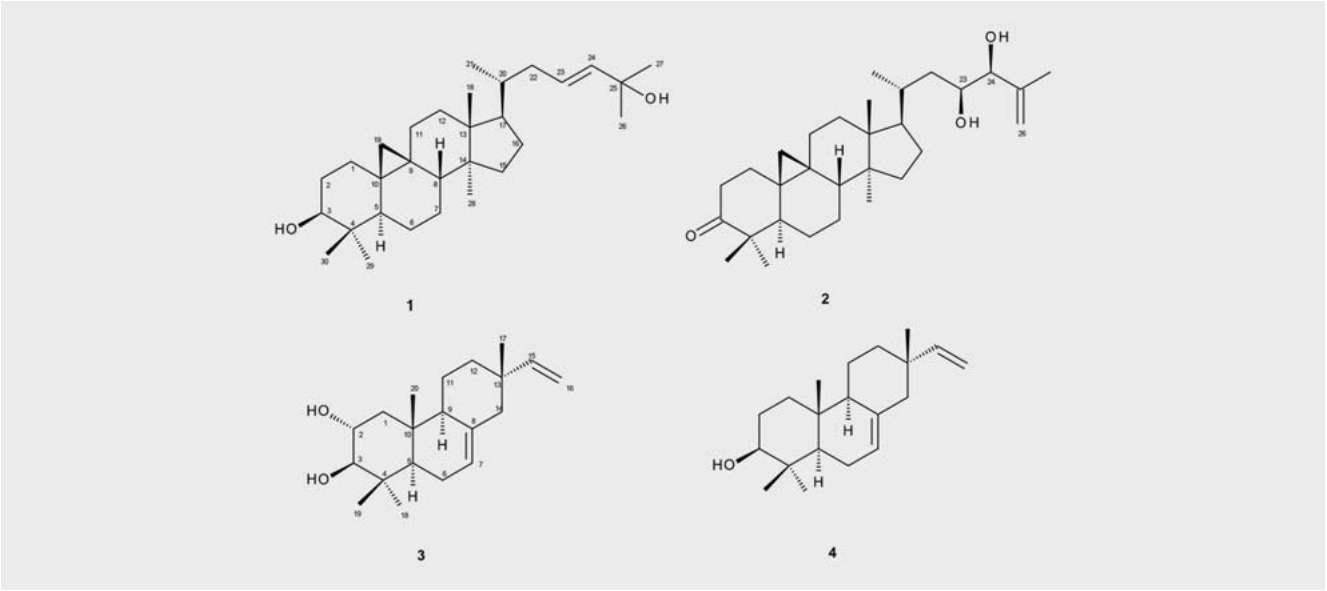

▶ **Fig. 1** Structures of compounds **1**–**4**.

cytotoxic compounds using bioactivity-guided fractionation followed by identification of these compounds using NMR and MS spectral analysis. Using this approach, we obtained four terpenoids: cycloart-23*E*-ene-3β,25-diol (**1**), (23S*,24S*)-dihydroxycicloart-25-en-3-one (**2**), isopimara-7,15-diene-2α,3β-diol (**3**), and isopimara-7,15-dien-3β-ol (**4**), in which **2** and **3** are new derivatives. The *in vitro* cytotoxic activity of compounds **1**–**4** on tumor cells was examined and the obtained results indicated that cycloartane **1** is the more active metabolite with IC_{50} values ranging from 18.3 to 63.5 µM. Furthermore, it was observed that compound **1** might induce intrinsic apoptosis in B16F10-Nex2 melanoma cells. Thus, the obtained results suggest that compound **1** could be considered a candidate drug for cancer therapy.

Results and Discussion

The EtOH extract from the leaves of *G. macrophylla* as well as the respective partitions (*n*-hexane and EtOAc) were incubated at 100 µg/mL with B16F10-Nex2 cells (murine melanoma), and their viabilities were determined by the MTT assay [5]. As a result, 40% of cell viability was observed in the EtOH crude extract with 26% of cell viability in the *n*-hexane phase after incubation, suggesting the presence of bioactive compounds. However, the EtOAc phase was inactive since no reduction of cell viability was observed at 100 and 200 µg/mL. Aiming for the isolation of active compounds, the *n*-hexane phase from the EtOH extract was subjected to bioactivity-guided fractionation procedures to afford two cycloartane triterpenes (**1** and **2**) and two isopimarane diterpenes (**3** and **4**). The structures of the isolated compounds (▶ **Fig. 1**) were fully characterized by NMR and MS data analysis as well as by comparison with those reported in the literature [3, 6].

Compound **2** was isolated as an amorphous white solid. Its IR spectrum showed characteristic absorption bands from O-H (3436 cm^{-1}), =C–H (3078 cm^{-1}), C=O (1724 cm^{-1}), and C=C (1680 cm^{-1}). HR-ESI-MS spectrum showed the quasi-molecular ion peak at *m/z* 479.3475 $[M + Na]^+$, indicative of the molecular formula $C_{30}H_{48}O_3$, with seven degrees of unsaturation. ^{1}H NMR spectrum showed two doublets δ 0.58 (J = 4.5 Hz) and 0.80 (J = 4.5 Hz) as well as peaks at δ 2.71 (dt, J = 13.9 and 6.3 Hz, H-2a) and δ 2.30 (ddd, J = 13.9, 4.3 and 2.3 Hz, H-2b), which are indicative of a cycloartan-3-one derivative [7]. This spectrum also showed five singlets attributed to methyl groups at δ 0.91 (H-28), 1.01 (H-18), 1.05 (H-29), 1.10 (H-30), and 1.77 (H-27) as well as one doublet at δ 0.89 (J = 6.4 Hz), assigned to H-21. The presence of two olefinic hydrogens at δ 4.99 (br s, H-26a) and 5.03 (br s, H-26b) as well as two oxymethine hydrogens at δ 3.76 (ddd, J = 11.0, 6.7 and 2.0 Hz, H-23) and 3.80 (d, J = 6.7 Hz, H-24) suggested the presence of a side chain closely related to that observed in euphonerin E, isolated from *Euphorbia neriifolia* [7]. The mutual coupling between H-23 and H-24 was observed in the COSY spectrum. ^{13}C and DEPT 135° NMR spectral data confirmed the occurrence of a cycloartan-3-one derivative due to the peaks at δ 216.6 and 29.7, assigned to a carbonyl group at C-3 and a methylene ring (C-19), as well as those at range δ 18.0–22.2, attributed to six methyl groups. Similarly, to those observed in euphonerin E, the signals of sp^2 carbons in the side chain were observed at δ 145.1 (C-24) and 112.9 (C-25), whereas two secondary hydroxyl groups at C-23 and C-24 were observed at δ 70.9 and 78.8, respectively. The hydrogen bearing carbon signals were assigned by analysis of the HSQC spectrum, and the correlations observed in the HMBC spectrum (▶ **Table 1**), especially those between the signal at δ 4.99/5.03 (H-26) and those at δ 145.1 (C-24), 112.9 (C-25), and 18.6 (C-27) as well as between the signal at δ 3.80 (H-24), δ 70.9 (C-23), and 112.9 (C-25), confirmed the planar structure of **2** as 23,24-dihydroxycycloart-25-en-3-one. Both configurations of C-23 and C-24 were deduced as *S* by comparison of chemical shift values and coupling constants of H-23

▶ **Table 1** ^{1}H and ^{13}C NMR data (500 and 125 MHz, $CDCl_3$, δ/ppm) for compounds **2** and **3**.

	2			**3**		
Position	**δ_H (*J* in Hz)**	**δ_C**	**HMBC**	**δ_H (*J* in Hz)**	**δ_C**	**HMBC**
1	1.71 m	33.4	C-2, C-3, C-5, C-19	1.15 m 2.15 m	45.1	C-2, C-3, C-5, C-10 C-2, C-3, C-5, C-10
2	2.30 ddd (13.9, 4.3, 2.3) 2.71 dt (13.9, 6.3)	37.4	C-1, C-10 C-1, C-4, C-10	3.71 ddd (11.7, 9.6, 4.2)	68.4	C-3, C-4
3	–	216.6	–	3.05 d (9.6)	83.7	C-2, C-4, C-18, C-19
4	–	50.2	–	–	38.9	–
5	1.71 m	48.4	C-3, C-4, C-7	1.25 m	49.9	C-3, C-7
6	1.59 m	21.5	C-4, C-10	1.97 m	23.1	C7, C-8, C-10
7	1.64 m	28.3	C-9	5.40 br s	121.3	C-5, C-9, C-14
8	1.61 m	47.8	C-10, C-11, C-14, C-28	–	135.2	–
9	–	21.1	–	1.73 m	51.8	C-7, C-20
10	–	26.0	–	–	36.5	–
11	1.28 m	25.8	C-10, C-13, C-19	1.56 m	20.1	C-8, C-13
12	1.29 m	35.5	C-13, C-14, C-18	1.49 m 1.37 m	35.9	C-9, C-14 C-9, C-14
13	–	45.4	–	–	36.8	–
14	–	48.7	–	2.16 m 1.96 m	45.8	C-7, C-9, C-15 C-7, C-9, C-15
15	1.68 m	32.8	C-14, C-28	5.81 dd (17.5, 10.8)	150.2	C-13, C-14, C-17
16	2.08 m	26.7	C-14, C-20	4.99 dd (17.5, 1.4) 4.90 dd (10.8, 1.4)	109.3	C-13, C-15 C-13, C-15
17	1.67 m	53.1	C-18, C-21, C-22	0.87 s	21.5	C-13, C-14, C-15
18	1.01 s	18.1	C-14, C-17	0.88 s	28.8	C-3, C-4, C-5, C-19
19	0.58 d (4.5) 0.80 d (4.5)	29.7	C-1, C-8, C-9, C-11 C-1, C-5, C-8, C-9, C-11	0.95 s	15.6	C-3, C-4, C-5
20	1.68 m	31.7	C-17	1.05 s	16.8	C-1, C-5
21	0.89 d (6.4)	18.0	C-17, C-22	–	–	–
22	1.51 m	39.8	C-17, C-21, C-24	–	–	–
23	3.76 ddd (11.0, 6.7, 2.0)	70.9	C-20, C-24, C-25	–	–	–
24	3.80 d (6.7)	78.8	C-23, C-25, C-26, C-27	–	–	–
25	–	145.1	–	–	–	–
26	4.99 br s 5.03 br s	112.9	C-24, C-27 C-24, C-27	–	–	–
27	1.77 s	18.6	C-24, C-25, C-26	–	–	–
28	0.91 s	19.3	C-13, C-14, C-15	–	–	–
29	1.05 s	22.2	C-3, C-4, C-5, C-30	–	–	–
30	1.10 s	20.7	C-3, C-4, C-5, C-29	–	–	–

and H-24 with those reported in the literature to similar derivatives [7–9]. To confirm, the ECD spectrum of **2** showed a negative Cotton effect at $\lambda = 295$ nm, similar to those reported in related compounds cycloart-3-one-16,23,24,25-tetrol [10] and euphorerin E [7]. Thus, the structure of **2** was elucidated as (23*S**,24*S**)-dihydroxycycloart-25-en-3-one.

Compound **3** was isolated as an amorphous white solid. Its IR spectrum showed characteristic absorption bands from O-H (3336 cm^{-1}) =C–H (2854 cm^{-1}), and C=C (1631 cm^{-1}). HR-ESI-MS spectrum showed the *quasi*-molecular ion peak at *m/z* 327.2287 $[M + Na]^+$, indicative of the molecular formula $C_{20}H_{32}O_2$, with five degrees of unsaturation. ^{1}H NMR spectrum showed signals of hydrogens linked to sp^2 carbons at δ 5.81 (dd, $J = 17.5$ and 10.8, H-15), 4.99 (dd, $J = 17.5$ and 1.4 Hz, H16a), 4.90 (dd, $J = 10.8$ and 1.4 Hz, H-16b), and 5.40 (br s, H-7), which were in association with the peaks assigned to methyl groups at δ 0.87 (H-17), 0.88 (H-18), 0.95 (H-19), and 1.05 (H-20), indicating the occurrence of a isopimara-7,15-diene derivative [2]. This spectrum also

▶ **Table 2** Cytotoxic activity of compounds **1**–**4** and positive control cisplatin against different tumor cell lines.

	IC_{50} µM (95% CI)				
Cell line *	**1**	**2**	**3**	**4**	**cisplatin**
B16F10-Nex2	58.9 (54.8–63.1)	82.9 (64.6–106.4)	> 100	> 100	> 100
A2058	60.7 (50.0–73.5)	56.8 (53.2–60.6)	> 100	> 100	42.9 (34.6–53.2)
MCF7	63.5 (60.0–67.0)	43.9 (38.9–49.4)	> 100	> 100	> 100
HL-60	18.3 (17.8–18.8)	27.7 (26.0–29.3)	> 100	102.4 (93.5–112.1)	21.2 (19.3–23.3)
HeLa	52.1 (45.4–59.7)	48.3 (43.7–53.1)	> 100	> 100	17.3 (14.8–20.2)

IC_{50} = 50% inhibitory concentration (µM); 95% CI = 95% confidence interval. * B16F10-Nex2: murine melanoma, A2058: human melanoma, MCF7: human breast cancer, HL-60: human promyelocytic leukemia, HeLa: human cervical carcinoma

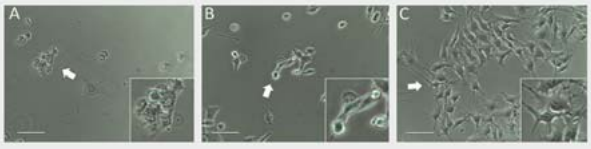

▶ **Fig. 2** Morphologic alterations in B16F10-Nex2 cells previously incubated with compound **1** at **A** 110 µM, **B** 55 µM, and **C** negative control for 18 h. White arrows indicate × 800 magnification inserts. Scale bar: 50 µm.

showed two coupled peaks at δ 3.71 (ddd, J = 11.7, 9.6 and 4.2 Hz) and 3.05 (d, J = 9.6 Hz), which could be assigned to H-3α and H-2β. Chemical shift values, splitting patterns, and coupling constants of these signals closely resembled those observed in isopirama-8(14),15-diene-7α-peroxy-2α,3β-diol, previously isolated from leaves of *G. macrophylla* [11], suggesting the same stereochemistry to C-2 and C-3 in both compounds. ^{13}C and DEPT 135° NMR spectral data confirmed this proposal due to the peaks of sp^2 carbons at δ 150.2 (C-15), 109.3 (C-16), 121.3 (C-7), and 135.2 (C-8) as well as the oxymethine carbons at δ 68.4 (C-2) and 83.7 (C-3). The hydrogen bearing carbon signals were assigned by analysis of the HSQC spectrum, and the correlations observed in the HMBC spectrum (▶ **Table 1**) confirmed the structure of **3** as isopimara-7,15-diene-2α,3β-diol.

Phytochemicals possess many therapeutic benefits, such as increased toleration, pharmacokinetic properties, and good solubility, indicating a greater likelihood for success in various phases of clinical trials with a good distribution in the human diet [12]. For that reason, it is very important to identify new bioeffective phytochemicals that have promising antitumor properties in order to develop novel strategies able to fight cancer. In this aspect, we evaluated the cytotoxic activity of isolated compounds **1**–**4** from *G. macrophylla* in several cancer cell lines. Compounds **3** and **4** were less active in comparison to compounds **1** and **2** in which no significant cytotoxicity was observed for compound **3** regarding melanoma, HeLa, A2058, and HL-60 cell lines, and compound **4** showed slight activity only against HL-60 cells. Compound **1** showed the highest cytotoxicity against most of the tested cancer cell lines, including the murine melanoma model, with IC_{50} values of 58.9 µM for B16F10-Nex2, 60.7 µM for A2058, 63.5 µM for MCF-7, 18.3 µM for HL-60, and 52.1 µM for HeLa cell lines (▶ **Table 2**).

Previous studies have demonstrated the cytotoxic activity of related cycloartane derivatives against a panel of human cancer cell lines, highlighting the potential of these compounds as antitumor agents [13]. Thus, based on this aspect and on the IC_{50} value determined in B16F10-Nex2 cells (58.9 µM) in comparison to the positive control cisplatin (> 100 µM), compound **1** was selected to propose the mechanism of action on this cell lineage. As melanoma is known for its chemoresistant properties, the development of new prototypes that induce cytotoxic effects in melanoma cells have been considered of great relevance for drug discovery and cancer therapy [14]. The morphology of tumor cells after *in vitro* treatments such as apoptosis, autophagy, necrosis, and further cell death types can provide important information concerning the fate of cells when they are incubated with cytotoxic concentrations of a drug, which helps to better clarify the tumor-induced cell death. Morphological classifications have dominated the cell death research scene even after the introduction of biochemical assays into the laboratory routine [15]. Compound **1** induced morphological changes in melanoma cells such as shrinkage of the cytoplasm, pyknotic chromatin, and a round shape of the cell structure given to pseudopods retraction as well as a reduced adhesion profile (▶ **Fig. 2**). These are well-known morphological hallmarks of apoptosis [16]. In addition, pyknotic chromatin can also be evidenced by condensation and fragmentation of the nucleus, which is a main feature of apoptosis [17]. Thus, it was also observed that compound **1** could induce significant condensation and specific fragmentation of the chromatin in melanoma-treated cells (▶ **Fig. 3A**) following Hoechst and terminal deoxynucleotidyl transferase dUTP nick end labeling (TUNEL) staining, respectively. Quantitatively, 46% of treated cells showed an

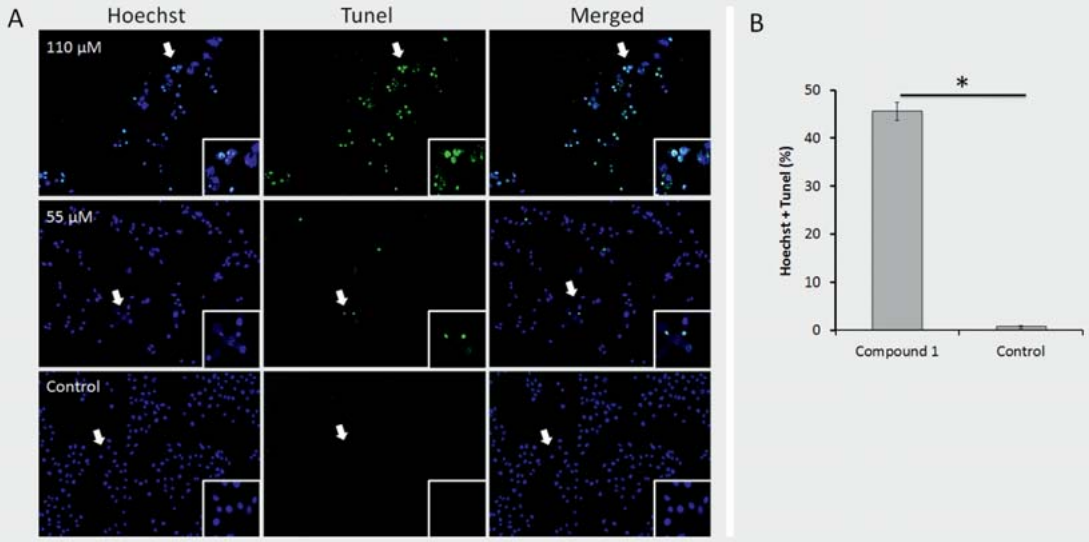

▶ **Fig. 3** Genomic DNA condensation and fragmentation induced by compound **1** in melanoma cells. **A** 1×10^4 B16F10-Nex2 cells were incubated with compound **1** at 110 µM and 55 µM for 18 h. Tumor cells were stained with Hoechst (blue) and TUNEL (green) for condensation and fragmentation quantification by image cytometry, respectively. **B** Percent ratio of double positive stained cells (Hoechst and TUNEL) treated with compound **1** at 110 µM and negative control. Results are described as the means of three individual experiments ± standard errors; * $p < 0.05$.

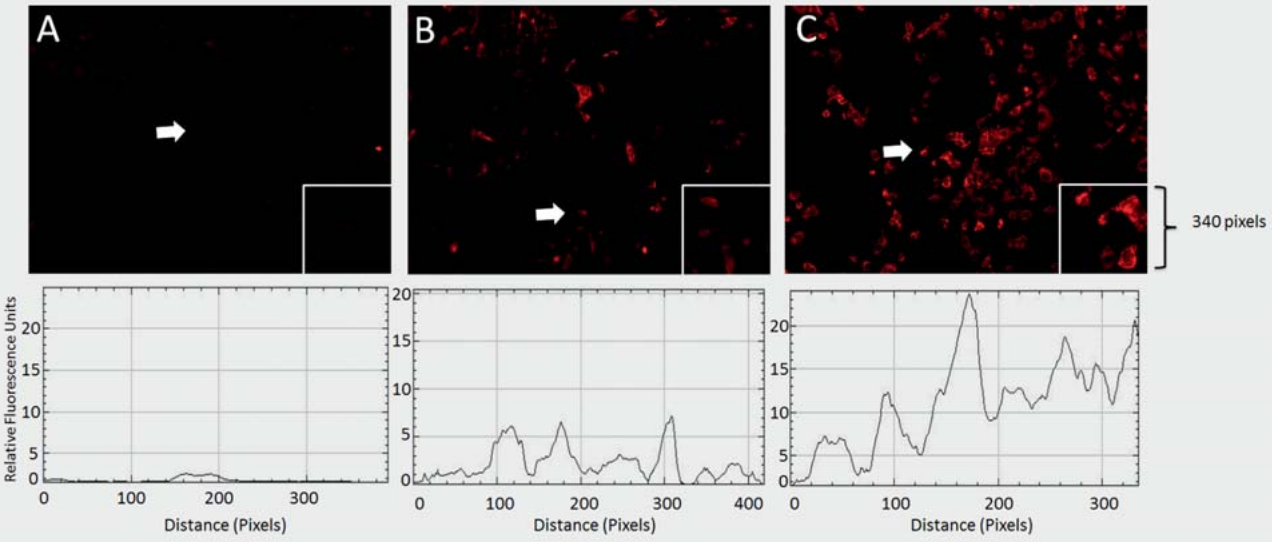

▶ **Fig. 4** Mitochondrial membrane potential investigation in melanoma cells treated with compound **1**. 1×10^4 B16F10-Nex2 cells were previously incubated with 5 nM of the mitochondrial membrane integrity probe TMRE treated with compound **1** at **A** 110 µM, **B** 55 µM, and **C** negative control. Below each figure, the relative fluorescence units profile of the areas indicated by white arrows and enhanced in 340 pixels inserts are shown. Relative fluorescence units are proportional to the mitochondrial membrane potential integrity, as indicated by increased fluorescence intensity of the mitochondrial probe TMRE.

overlap between condensation and fragmentation processes (▶ **Fig. 3 B**). In addition, the TUNEL assay has been designed to detect exclusive apoptotic cells that undergo extensive DNA fragmentation during the late stages of apoptosis [18]. The intrinsic pathways that start apoptosis involve several non-receptor-mediated stimuli that target mitochondria [16], causing the loss of the mitochondrial transmembrane potential and release of proapoptotic proteins from the intermembrane space into the cytosol

[19]. It was observed that compound **1** was also able to decrease the mitochondrial transmembrane potential in B16F10-Nex2 melanoma cells, evidenced by a dose-dependent reduction of tetramethylrhodamine ethyl ester (TMRE) fluorescence staining (▶ **Fig. 4A**), and quantified as fluorescence relative units in treated groups in comparison with a negative control (▶ **Fig. 4B**).

All the evidence suggests that compound **1**, and similar analogues with the same range of biological activity, may act on tumor cells by inducing intrinsic apoptosis in melanoma cells, which are known to be very resistant to apoptotic process, and for that reason, they should be considered for further elucidation of the complete mechanism of action against melanoma cells to be developed as promising therapeutic drugs in cancer therapy.

Material and Methods

General

Silica gel (Merck, 230–400 mesh), Florisil (Sigma-Aldrich), and Sephadex LH-20 (Sigma-Aldrich) were used for column chromatographic separation procedures, while silica gel 60 PF_{254} (Merck) was used for analytical TLC (0.25 mm). HPLC was performed using a Dionex Ultimate 3000 chromatograph with a UVD-DAD 170 V as the detector using a Luna Phenomenex C_{18} column (10 × 250 mm, particle and pore size of 5 µm and 175 Å, respectively) in the semi-preparative mode or Dionex C_{18} (4.6 × 250 mm, particle and pore size of 5 µm and 120 Å, respectively) in the analytical mode. ^{1}H, ^{13}C, DEPT 135°, COSY, HSQC, and HMBC NMR spectra were recorded on a Bruker Avance III 500 and Ultrashield 300 Advance III spectrometers operating at 500/300 and 125/75 MHz to the ^{1}H and ^{13}C nucleus, respectively. $CDCl_3$ (Aldrich) was used as the solvent and the residual peak of the nondeuterated solvent was used as the internal standard. Chemical shifts (δ) are reported in ppm and the coupling constant (J) in Hz. IR spectra were obtained on a Bomem MB-100 spectrometer. HR-ESI-MS spectra were recorded on a Bruker MicroTOF-QII using electrospray ionization in the positive mode and LR-EI-MS were measured with an HP 5990/5988A mass spectrometer. Optical rotations were measured on a digital polarimeter Jasco DIP-370 (Na filter, λ = 588 nm) and electronic circular dichroism (ECD) analysis was performed using MeOH on a JASCO J-720 spectropolarimeter.

Plant material

G. macrophylla leaves were collected from a single specimen at the Instituto de Biociências, Universidade de São Paulo, São Paulo State, Brazil in January 2014. The specimen was identified by MSc. Guilherme de M. Antar (Departamento de Botânica, Instituto de Biociências, Universidade de São Paulo) and a voucher specimen (ANTAR 1397) has been deposited in the Herbarium of the Universidade de São Paulo, SPF.

Extraction and isolation

The dried and powdered leaves (1.8 kg) of *G. macrophylla* were extracted with *n*-hexane (10 × 800 mL) and then exhaustively extracted with EtOH (20 × 1000 mL). After concentration under reduced pressure, 11.8 and 130.0 g of *n*-hexane and EtOH extracts were obtained, respectively. Part of the EtOH extract (70 g) was resuspended in EtOH : H_2O (1 : 2, 500 mL) and sequentially partitioned using *n*-hexane and EtOAc to afford 18.5 and 10.1 g of each organic phase. As cytotoxic activity was detected in the *n*-hexane phase, part of this material (18.0 g) was chromatographed on a silica gel column (750 × 50 mm, 125 mL fractions) eluted with increasing amounts of EtOAc in *n*-hexane (9 : 1, 8 : 2, 7 : 3, 1 : 1, 3 : 7, 2 : 8, and 1 : 9). This chromatographic step afforded 15 fractions (A–O) in which bioactivity was detected in fractions F, H, I, and K. Fraction F (3095 mg) was chromatographed on a silica gel column (500 × 25 mm, 10 mL fractions) eluted with increasing amounts of EtOAc in *n*-hexane (8 : 2, 7 : 3, 1 : 1, 3 : 7, 2 : 8, and 1 : 9) to give 17 fractions (F1–F17). As bioactivity was concentered in fraction F6 (215 mg), this material was subjected to fractionation over Sephadex LH-20 (300 × 25 mm, 10 mL fractions) eluted with MeOH to afford four fractions (F6/1-F6/4) in which bioactivity was detected in fractions F6/2 and F6/3. These fractions were pooled together since they were composed of similar material, as observed by NMR. Thus, the obtained group of fractions (77.5 mg) was purified by HPLC (MeOH : H_2O, 9 : 1, 2.5 mL/min, λ = 218 nm) to afford 2.0 mg of **4** (99% of purity). Fraction H (915 mg) was chromatographed on a silica gel column (500 × 25 mm, 10 mL fractions) eluted with increasing amounts of EtOAc in hexane (9 : 1, 8 : 2, 7 : 3, 1 : 1, 3 : 7, 2 : 8, 1 : 9, and pure EtOAc) to give six fractions (H1–H6). Fraction H3 (303 mg), active, was subjected to fractionation over a Florisil column (500 × 25 mm, 10 mL fractions) eluted with increasing amounts of MeOH in $CHCl_3$ (pure $CHCl_3$, 9 : 1, 8 : 2, 7 : 3, 1 : 1, 3 : 7, 2 : 8, 1 : 9, and pure MeOH) to give five fractions (H3/1-H3/5). As bioactivity was detected in fraction H3/2 (195 mg), this material was purified by preparative TLC (silica gel, CH_2Cl_2 : Me_2CO 95 : 5) to afford 22.1 mg of **1** (98% of purity). Fraction I (529 mg) was chromatographed on a silica gel column (500 × 25 mm, 10 mL fractions) eluted with increasing amounts of EtOAc in hexane (9 : 1; 8 : 2; 7 : 3; 1 : 1; 3 : 7; 2 : 8; 1 : 9 and pure EtOAc) to give eight fractions (I1–I8). Fraction I3 (285 mg), active, was subjected to fractionation over Sephadex LH-20 (300 × 25 mm, 10 mL fractions) eluted with MeOH to afford three fractions (I3/1-I3/3) in which bioactivity was detected in fraction I3/1 (223 mg). This fraction was subjected to fractionation over a Florisil column (500 × 25 mm, 10 mL fractions) eluted with increasing amounts of MeOH in CH_2Cl_2 (pure CH_2Cl_2, 9 : 1, 8 : 2, 7 : 3, 1 : 1, 3 : 7, 2 : 8, 1 : 9, and pure MeOH) to give three fractions (I3/1-1-I3/1–3). As bioactivity was detected in fraction I3/1–2 (31 mg), this material was purified by preparative TLC (silica gel, *n*-hexane : EtOAc 9 : 1) to afford 2.5 mg of **2** (98% of purity). Fraction K (502 mg) was chromatographed on a silica gel column (500 × 25 mm, 10 mL fractions) eluted with increasing amounts of EtOAc in hexane (9 : 1, 8 : 2, 7 : 3, 1 : 1, 3 : 7, 2 : 8, 1 : 9, and pure EtOAc) to give nine fractions (K1–K9). Fraction K5 (295 mg), active, was subjected to fractionation over a silica gel column (300 × 25 mm, 10 mL fractions) eluted with increasing amounts of EtOAc in hexane (8 : 2, 7 : 3, 1 : 1, 3 : 7, 2 : 8, and 1 : 9) to afford seven fractions (K5/1-K5/7) in which bioactivity was detected in fraction K5/4 (41 mg). This material was purified by preparative TLC (silica gel, *n*-hexane : EtOAc 1 : 1) to afford 2.5 mg of **3** (99% of purity).

(23S,24S*)-Dihydroxycycloart-25-en-3-one* (**2**): Amorphous white solid. $[\alpha]_D^{25}$ + 89.5 (*c* 0.002, EtOAc); ^{1}H NMR and ^{13}C NMR, see ▶ **Table 1**. IR (film) ν_{max} 3436, 2840, 1724, 1707, 1035 cm^{-1};

HR-ESI-MS: *m/z* 479.3475 $[M + Na]^+$ (calcd. for $C_{30}H_{48}O_3Na$, 479.3501).

Isopimara-7,15-dien-2α,3β-diol (**3**). Amorphous white solid. $[\alpha]_D^{25}$ + 22.2 (*c* 0.001, EtOAc); ^1H NMR and ^{13}C NMR, see ▶ **Table 1**. IR (film) ν_{max} 3336, 2854, 1731, 1350, 1058 cm^{-1}; HR-ESI-MS: *m/z* 327.2287 $[M + Na]^+$ (calcd. for $C_{20}H_{32}O_2Na$, 327.2299).

Cell lines and culture conditions

The murine melanoma cell line B16F10-Nex2 is a melanotic, aggressive subline derived from an original B16F10 melanoma cell line provided by the Ludwig Institute for Cancer Research (LICR), São Paulo branch, and was established at the Experimental Oncology Unit, Federal University of São Paulo (UNIFESP), and deposited in the *Banco de Células do Rio de Janeiro* (BCRJ), reg. 0342. Human cancer cell lines melanoma A2058, breast cancer MCF-7, cervical cancer HeLa, and human promyelocytic leukemia HL-60 were provided by the LICR. Cells were cultivated as previously described [20].

Cell viability assay

Crude extract, partition phases, fractions, and isolated compounds **1–4** were incubated with 1×10^4 murine and human tumor cells for 24 h at different concentrations ranging from 0 to 100 µg/mL. Cell viability was determined by using the colorimetric MTT (Sigma) assay: 10 µL of MTT solution (5 mg/mL) were added to each well and incubated at 37 °C for 4 h. Next, 100 µL of 10% SDS were added to each sample and incubated at 37 °C for 24 h. Readings were performed in a microplate reader (Spectramax M2e) at 570 nm. IC_{50} values were quantified using GraphPad Prism 5 software to build the nonlinear fit log transformation to acquire the IC_{50} values and confidence intervals (CI). Cisplatin was used as a positive drug control and all experiments were performed in triplicate.

DNA condensation and fragmentation assay

B16F10-Nex2 cells (1×10^5) were seeded in black 96-well plates with a flat transparent bottom in the presence of compound **1** at 110 µM and 55 µM at 37 °C for 18 h. After the incubation period, the cells were washed two times in PBS 1 ×, and incubated with the DNA condensation blue probe Hoechst 33342 (Invitrogen) and the green DNA fragmentation probe TUNEL (Roche) following the manufacturer instructions. Cells were analyzed and quantified by image cytometry using the Cytell image system platform (GE Healthcare).

Mitochondrial transmembrane potential (Δψm) assay

B16F10-Nex2 cells (1×10^4) were seeded in black 96-well plates with a flat transparent bottom in the presence of 5 nM of TMRE (Molecular Probes) for 30 min at 37 °C with 5% CO_2. Subsequently, 110 µM and 55 µM of compound **1** and the negative control were administered to the cells for 18 h. Then, images were acquired and analyzed by image cytometry using the Cytell image system platform (GE Healthcare).

Statistical analysis

The results are represented by the mean and standard deviation of triplicate samples from at least two independent assays. The IC_{50} values were calculated using sigmoid dose-response curves in Graph Pad Prism 4.0 software. Student's t-test was used for statistical analysis of all *in vitro* mechanism assays and $p < 0.05$ was considered a significant difference between experimental groups and controls.

Supporting information

NMR and MS spectra of compounds **1–4** as well as dose-dependent column graphs are available as Supporting Information.

Acknowledgements

This work was funded by grants and fellowships provided by Fundação de Amparo a Pesquisa do Estado de São Paulo (FAPESP – projects 2014/08961-2 and 2015/11936-5). We also thank CNPq for the scientific research award to J. H. G. L.

Conflict of Interest

The authors declare no conflict of interest.

References

[1] Correa MP. Dicionário de Plantas Úteis e das Exóticas Cultivadas, Vol. 1. Rio de Janeiro: Ministério da Agricultura; 1984

[2] Lago JHG, Brochini CB, Roque NF. Terpenes from leaves of *Guarea macrophylla* (Meliaceae). Phytochemistry 2000; 55: 727–731

[3] Lago JHG, Roque NF. Cycloartane triterpenoids from *Guarea macrophylla*. Phytochemistry 2002; 60: 329–332

[4] Morais TR, Coutinho AP, Camilo FF, Martins T, Sartorelli P, Massaoka M, Figueiredo CR, Lago JHG. Application of an ionic liquid in the microwave assisted extraction of cytotoxic metabolites from fruits of *Schinus terebinthifolius* Raddi (Anacardiaceae). J Braz Chem Soc 2017; 28: 492–497

[5] Girola N, Figueiredo CR, Farias CF, Azevedo RA, Ferreira AK, Teixeira SF, Capello TM, Martins EGA, Matsuo AL, Travassos LR, Lago JHG. Camphene isolated from essential oil of *Piper cernuum* (Piperaceae) induces intrinsic apoptosis in melanoma cells and displays antitumor activity *in vivo*. Biochem Biophys Res Commun 2015; 467: 928–934

[6] Lago JHG, Roque NF. Estudo fitoquímico da madeira de *Guarea macrophylla* (Meliaceae). Quím Nova 2009; 32: 2351–2354

[7] Toume K, Nakazawa T, Ohtsuki T, Arai MA, Koyano T, Kowithayakorn T, Ishibashi M. Cycloartane triterpenes isolated from *Combretum quadrangulare* in a screening program for death-receptor expression enhancing activity. J Nat Prod 2011; 74: 249–255

[8] Toume K, Nakazawa T, Hoque T, Ohtsuki T, Arai MA, Koyano T, Kowithayakorn T, Ishibashi M. Cycloartane triterpenes and ingol diterpenes isolated from *Euphorbia neriifolia* in a screening program for death-receptor expression-enhancing activity. Planta Med 2012; 78: 1370–1377

[9] Mohamad K, Martin MT, Leroy E, Tempete C, Sevenet T, Awang K, Païs M. Argenteanones C–E and argenteanols B–E, cytotoxic cycloartanes from *Aglaia argentea*. J Nat Prod 1997; 60: 81–85

[10] Herz W, Watanabe K, Kulanthaivel P, Blunt FJ. Cycloartanes from *Lindheimera texana*. Phytochemistry 1985; 24: 2645–2654

[11] Lago JHG, Roque NF. New diterpenoids from leaves of *Guarea macrophylla* (Meliaceae). J Braz Chem Soc 2005; 16: 643–646

[12] Aggarwal BB, Sethi G, Baladandayuthapani V, Krishnan S, Shishodia S. Targeting cell signaling pathways for drug discovery: an old lock needs a new key. J Cell Biochem 2007; 102: 580–592

[13] Ma YY, Zhao DG, Li Y, Chen JJ, Zeng J, Zhao QQ, Gao K. Cytotoxic triterpenes with diverse skeletons from *Amoora tsangii*. Phytochem Lett 2016; 15: 251–255

[14] Grossman D, Altieri DC. Drug resistance in melanoma: mechanisms, apoptosis, and new potential therapeutic targets. Cancer Metastasis Rev 2001; 20: 3–11

[15] Galluzzi L, Vitale I, Abrams JM, Alnemri ES, Baehrecke EH, Blagosklonny MV, Dawson TM, Dawson VL, El-Deiry WS, Fulda S, Gottlieb E, Green DR, Hengartner MO, Kepp O, Knight RA, Kumar S, Lipton SA, Lu X, Madeo F, Malorni W, Mehlen P, Nuñez G, Peter ME, Piacentini M, Rubinsztein DC, Shi Y, Simon HU, Vandenabeele P, White E, Yuan J, Zhivotovsky B, Melino G, Kroemer G. Molecular definitions of cell death subroutines: recommendations of the Nomenclature Committee on Cell Death 2012. Cell Death Differ 2012; 19: 107–120

[16] Elmore S. Apoptosis: a review of programmed cell death. Toxicol Pathol 2007; 35: 495–516

[17] Kroemer G, Galluzzi L, Vandenabeele P, Abrams J, Alnemri ES, Baehrecke EH, Blagosklonny MV, El-Deiry WS, Golstein P, Green DR, Hengartner M, Knight RA, Kumar S, Lipton SA, Malorni W, Nuñez G, Peter ME, Tschopp J, Yuan J, Piacentini M, Zhivotovsky B, Melino G. Classification of cell death: recommendations of the Nomenclature Committee on Cell Death 2009. Cell Death Differ 2009; 16: 3–11

[18] Kyrylkova K, Kyryachenko S, Leid M, Kioussi C. Detection of apoptosis by TUNEL assay. Methods Mol Biol 2012; 887: 41–47

[19] Saelens X, Festjens N, Vande Walle L, van Gurp M, Van Loo G, Vandenabeele P. Toxic proteins released from mitochondria in cell death. Oncogene 2004; 23: 2861–2874

[20] Figueiredo CR, Matsuo AL, Azevedo RA, Massaoka MH, Girola N, Polonelli L, Travassos LR. A novel microtubule de-stabilizing complementarity-determining region C36L1 peptide displays antitumor activity against melanoma *in vitro* and *in vivo*. Sci Rep 2015; 5: 14310–14327